Mapping of Depth to Basement in Masu Area of Nigerian Sector of Chad Basin, Using Aeromagnetic and Aerogravity Data.

Akiishi, M., Isikwue, B. C. and Tyovenda, A. A.
Department of Physics, Federal University of Agriculture Makurdi, Benue State, Nigeria
Corresponding Author: Isikwue, B. C

Abstract: *This work maps the depth to basement in Masu area, which is located in the Nigerian sector of Chad basin (Lat. 12° 00' - 13° 00' N and Long. 12° 30' - 14° 00' E), using source parameter imaging and spectral analysis techniques. Application of minimum curvature in gridding the total magnetic field intensity and Bouguer anomaly data was done using the Oasis Montaj 6.4.2 software. First order polynomial fitting was applied in Regional - residual separation. Both residual magnetic intensity and residual gravity maps show the existence of intrusive bodies in the eastern part of Masu. From the aeromagnetic result, the depth to basement estimated using source parameter imaging (SPI) ranges from 479.9 (shallow magnetic bodies) to 6507.6 m (deep lying magnetic bodies) m, while the depths estimated from the source parameter imaging (SPI) of the aerogravity data range from 1140.6 (shallow gravity bodies) to 5879.4 m (deep lying gravity bodies). On the other hand, the depth to basement obtained via spectral analysis using aeromagnetic data ranges from 0.661 to 6.173 km, while that obtained using aerogravity data varies from 0.361 to 5.896 km. The highest depth to basement is obtained by source parameter imaging using aeromagnetic data. On the other hand, the highest depth to basement is obtained by spectral analysis technique using aerogravity data. The sedimentary thicknesses of 6507.6 and 5879.4 m show sufficiently thick sediments suitable for hydrocarbon accumulation. This implies that the area has the potential for hydrocarbons exploration.*

I. Introduction

The Earth's subsurface contains natural resources, which include hydrocarbon, mineral deposits, rocks, underground water and so on.[13] Over the years, the search for subsurface natural resources especially mineral deposits and hydrocarbon potential has become a major concern to geophysicists, geologists and exploration scientists. A large portion of the country's revenue comes from export and domestic sale of petroleum and minerals deposits.

A lot of geophysical explorations have been carried out in the Niger Delta area of Nigeria, hence the fear that soon or later the economic reserve of the country from such area may have hitch due to depletion in the hydrocarbon potentials and mineral deposits. Therefore, the need to investigate the economic minerals and hydrocarbon potentials of other geologic provinces, particularly the Nigerian sector of Chad Basin which is one of the inland Basins in Nigeria presumed to have high hydrocarbon potential aside other Earth minerals with high economic values.

There is the possibility that hydrocarbon potential and other economic mineral deposit might be found in the Nigerian sector of Chad Basin following the discoveries of hydrocarbon potentials and other mineral deposits in the neighboring countries such as republic of Niger, Chad, Sudan and Libya which have similar geological structural setting as that of the Nigerian sector of Chad Basin. Secondly, the possession of the Nigerian sector of Chad Basin of some favorable features such as age of the Basin, thickness of structurally related trap which encourages

accumulation of hydrocarbon potential call for its geophysical investigation.[1] In addition, the order by the federal government of Nigeria that national petroleum cooperation (NNPC) should resume exploration activities in the Nigerian Chad Basin, triggered off the interest to investigate this sedimentary Basin.[15]
Some researchers have carried out depth to basement estimation using source parameter imaging in other areas of the Nigerian sector of Chad Basin and not singly on Masu.[2,3,4,12,17,18,19,21,22,23,28,31,32,33] Moreover, these works were carried out using low resolution aeromagnetic data of 1974 and 1980. In addition, some of the works were carried using land survey measurement, which could be restricted in some areas due to differences in topography, thus not giving adequate information of the area.

Therefore, there is need to use a high resolution airborne data which will not only provide the capability of traversing regions that were otherwise difficult or impossible to cover by land survey geophysical methods, but will produce a much more detailed and better resolved picture of the geologic structures in the

----

area. In addition, since no work has been known before now to be carried out using aerogravity data in the area, there is need to use two or more geophysical methods to investigate the area. This is because; the limitation of one method may be compensated for by the other method, thereby, giving a better result that could be used to map out subsurface area of the location. This research is very useful for a reconnaissance survey for oil and mineral deposits in the area. Hence, the result from the work could be used to suggest portions of hydrocarbon and mineral presence in the area as well as the possible depths of assessment.

Location and geology of the study area

The study area, Masu is located in Nigerian sector of Chad Basin. The Chad basin lies within latitude 12° 00' to 13° 00' North and longitude 12° 30' to 14° 00' East (Fig.1). It lies within a vast area of central and West Africa at an elevation between 200 and 500 m above sea level and covers approximately 230,000 km². [4] It is the largest area of inland drainage in Africa. [8,10,20] It extends into parts of the republic of Niger, Chad, Cameroon, Nigeria and Central Africa. The Nigerian Chad Basin is about one tenth of the basin and has a broad sediment-filled depression spanning north eastern Nigeria and adjoining parts of the Republic of Chad.
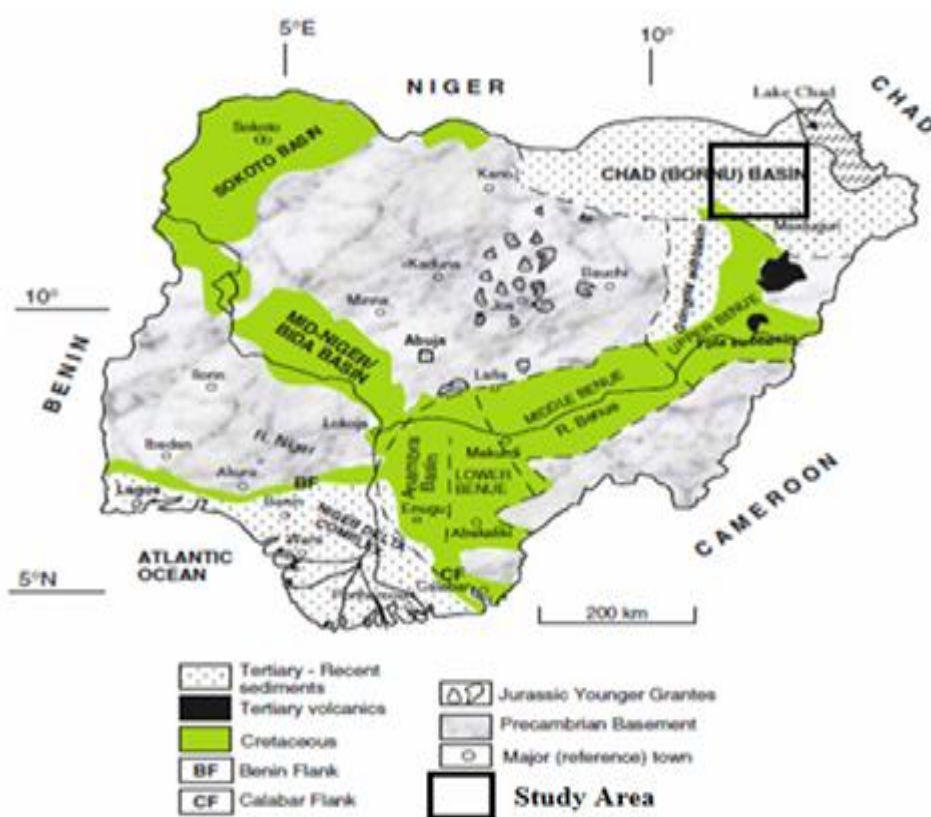

Figure 1: The Map of Nigeria Showing the Location of Chad Basin.[26]

The area generally is endowed with rock mineral base resources such as clay, salt, limestone, kaolin, iron ore, uranium, mica etc.[4] The sedimentary rocks of the area have cumulative thickness of over 3.6 km and the rocks consist of thick basal continental sequence overlaid by transitional beds followed by a thick succession of quaternary Limnic, fluviatile and eolian sand, clay etc.[29]

The stratigraphic sequence (Table1) shows that Chad, Kerri-Kerri and Gombe formations have an average thickness of 130 to 400 m. Below this formations are the Fika shale with a dark grey to black in colour, with an average thickness of 430 m. Others are Gongila and Bima formations with average thicknesses of 320 and 3500 m, respectively.[29,30]

Table 1: Generalized Stratigraphic Sequence of Nigerian Chad Basin.[31]

Age	Formations	Lithology	Depositional Environment	Thickness (m)**	INDEX
Pliocene-Pleistocene	Chad		Continental (Lacustrine)	50 – 425	Sand; Clay; Claystone; Limestone; Siltstone; Coal; Shale; Sandstone; Igneous sills; Basement rocks; Unconformity; ** Thickness from well logs
Paleocene	Kerri-Kerri		Continental	455 – 545	
Maastric -htian	Gombe Sandstone		Deltaic, Estuarine	301 – 402	
Turonian-Santonian	Fika Shale		Shallow marine	606 – 2012	
Turonian	Gongila		Marine, Estuarine (Transitional)	226 – 1363	
Albian-Cenomanian	Bima		Continental	408 – 1397	
Pre-Cambrian			Crystalline Basement		

II. Material And Methods

Source of Data

The high resolution airborne magnetic and gravity data used for this study were obtained from Nigerian Geological Survey Agency (NGSA). The airborne gravity data were obtained in 2013 using GRACE GRAVITY MODEL Sensor onboard 2 satellites by National Aeronautics and Space Administration (NASA) and German Aerospace Center, while the aeromagnetic data were obtained using a 3 x Scintrex CS2cesium vapour magnetometer by Fugro Airborne Surveys in 2009. The airborne magnetic survey was carried out at 80 m elevation along flight lines spaced 500 m apart. The flight line direction was 135°, while the tie line direction was 225°. A correction based on the international Geomagnetic Reference Field (IGRF) 2010 was applied.

Theory of Source Parameter Imaging

The source parameter imaging (SPI) uses an extension of the complex analytical signal to estimate magnetic source depths, source geometries, the dip and susceptibility contrast. It has the advantage of producing a more complete set of coherent solution points and it is easier to use than other depth mapping techniques such as the Euler deconvolution technique.

The method estimates the depth from the local wave number of the analytical signal. The analytical signal $A_1(x, z)$ is defined by [22] as:

$$A_1(x,z) = \frac{\partial M(x,z)}{\partial x} - j\frac{\partial M(x,z)}{\partial z} \qquad (1)$$

where, M(x, z) is the magnitude of the anomalous field, j is the imaginary number, and z and x are Cartesian coordinates for the vertical and the horizontal directions perpendicular to strike, respectively. [22] showed that the horizontal and vertical derivatives comprising of the real and imaginary parts of the 2D analytical signal are related by the expression,

$$\frac{\partial M(x,z)}{\partial x} \Leftrightarrow -j\frac{\partial M(x,z)}{\partial z} \qquad (2)$$

where the ⇔ denotes a Hilberts transform pair. The Local wave number K_1 is defined [38] as:

$$k_1 = \frac{\partial}{\partial x}tan^{-1}\left[\frac{\partial M}{\partial z}\Big/\frac{\partial M}{\partial x}\right] \qquad (3)$$

The analytic signal involves second order derivative of total field, if used in a manner similar to that used by. [16] The Hilbert transform and the vertical derivative operator are linear, so the vertical derivative of equation (2) will give the Hilbert transform pair.

Thus, the analytic signal could be defined based on second-order derivatives, $A_2(x, z)$, where

$$A_2(x,z) = \frac{\partial^2 M(x,z)}{\partial z \partial x} - j\frac{\partial^2 M(x,z)}{\partial^2 z} \qquad (4)$$

This gives rise to a second-order local wave number K_2, where

$$K_2 = \frac{\partial}{\partial x} tan^{-1}\left[\frac{\partial^2 M}{\partial^2 z} / \frac{\partial^2 M}{\partial z \partial x}\right] \qquad (5)$$

Thus, the expressions in equations 3 and 5 imply that the SPI utilizes the relationship between source depth and the local wave number (K) of the observed field, which can be calculated for any point within a grid of data via horizontal and vertical gradients.[38]

Theory of spectral analysis

Spectral analysis is the process of calculating and interpreting the spectrum of potential field data. It has been used extensively over the years to derive depth to certain geological features [37]or the Curie isotherm.[36] The spectral depth method is based on the principle that a magnetic field measured at the surface can be considered as an integral of magnetic signature from all depths.[34] The Discrete Fourier Transform is the mathematical tool for spectral analysis and applied to regularly spaced data such as the aeromagnetic data. A Fast Fourier Transform (FFT) algorithm computes the Discrete Fourier Transform (DFT) of a sequence, or its inverse. The Fourier Transform is represented mathematically as [32]:

$$Y_i(x) = \sum_{n=1}^{N}\left[a_n \cos\left(\frac{2\pi n x_i}{L}\right) + b_n \sin\left(\frac{2\pi n x_i}{L}\right)\right] \qquad (6)$$

where, $Y_i(x)$ is the reading at x_i position, L is length of the cross-section of the anomaly, n is harmonic number of the partial wave number, N is number of data points, a_n is real part of the amplitude spectrum and b_n is imaginary part of the amplitude spectrum; for $i = 0, 1, 2, 3, ..., n$.
The logarithms of the energy spectrum (Log E) are plotted against the domain frequency. Two linear segments are drawn from each graph; and their gradients (m) are used to estimate the deep depth (D_1) and the shallow depth (D_2) as shown equations 7 - 9.

$$Slope\ (m_1, m_2) = \frac{Log\ Energy}{Frequency} \qquad (7)$$

$$D_1 = -\frac{m_1}{4\pi} \qquad (8)$$

$$D_2 = -\frac{m_2}{4\pi} \qquad (9)$$

where, m_1 and m_2 are slopes of the first and second segment of the plot and the negative sign (-) indicates depth to the subsurface.

Methods

The total magnetic intensity and Bouguer anomaly data were separately imported into Oasis Montaj 6.4 software and were subsequently gridded using minimum curvature. These gridded data were further used to produce the total magnetic intensity and Bouguer anomaly maps. The regional - residual separation was carried out by first order polynomial fitting. The residual values of both magnetic and Bouguer anomalies were used to produce the residual magnetic intensity and residual gravity anomaly maps.

Source parameter imaging

The first and second order local wave numbers were used to determine the most appropriate model and depth estimate of any assumption about a model. Oasis Montaj software was employed to compute the SPI image and depth using equations (1) – (5)

Spectral analysis

The residual magnetic and residual gravity maps were divided into 9 equal spectral cells using the filtering tool of the Microsoft excel software. Each profile covers a square area of 18.33 by 18.33 km. Fast Fourier Transform (FFT) technique(equation 6) was employed in Microsoft (MS) excel program to transform the gravity and magnetic data into the radial energy spectrum for each block. The average radial energy spectra were calculated and displayed in a logarithm figure of energy versus frequency. The slopes obtained from equation 7 were further substituted in to equations 8 and 9 to estimate two depths (D_1 and D_2) for each of the nine spectral cells.

III. Result

Figure 2 presents the results of different qualitative interpretational stages of gravity and magnetic data. These are: (a) Total magnetic intensity map, (b) Bouguer anomaly map, (c) residual magnetic intensity

map and (d) is residual Bouguer anomaly map. On the other hand, Figure 3 gives the results of the quantitative interpretation using source parameter imaging to map the depth to basement. These are shown in (a) sources parameter imaging aeromagnetic map and (b) source parameter imaging aerogravity map. From the spectral analysis, Tables 2 and 3 present the estimated depths (Deep and shallow) for both aeromagnetic and aerogravity data respectively. Finally, Figure 4 gives the 2-D contour maps for the following (a) aeromagnetic deep depths to basement (b) aeromagnetic shallow depths to basement (c) aerogravity deeps depth to basement and (d) aerogravity shallow depths to basement.
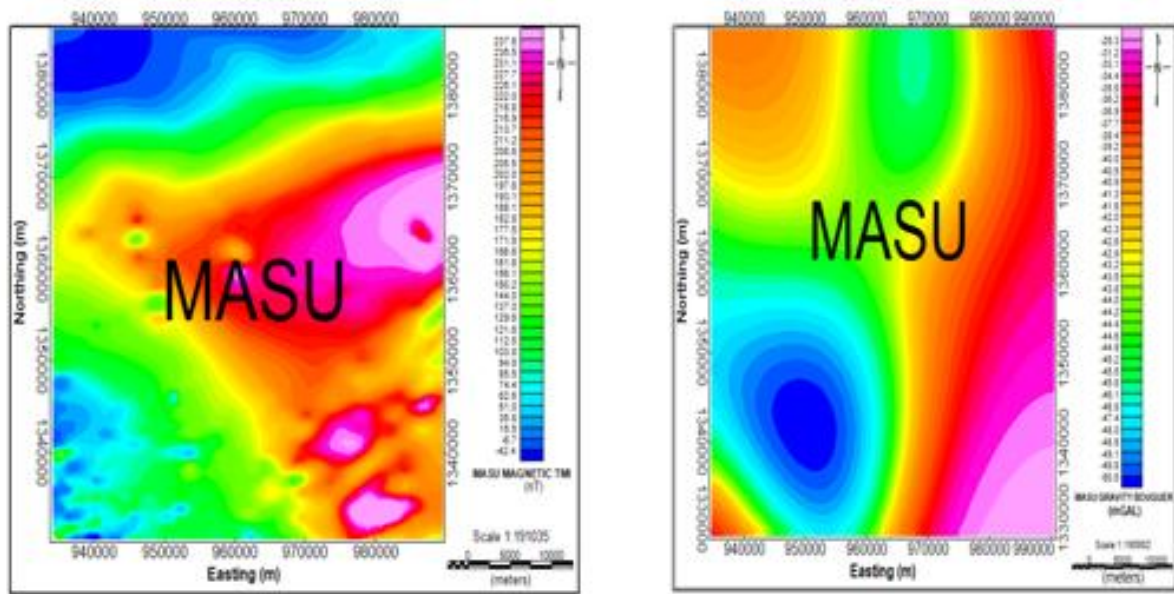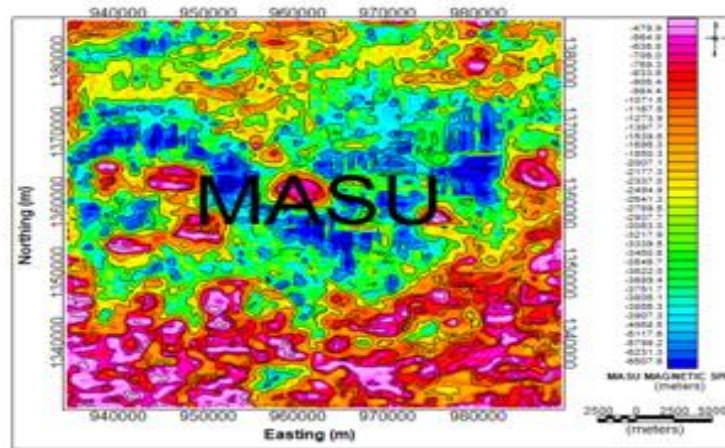

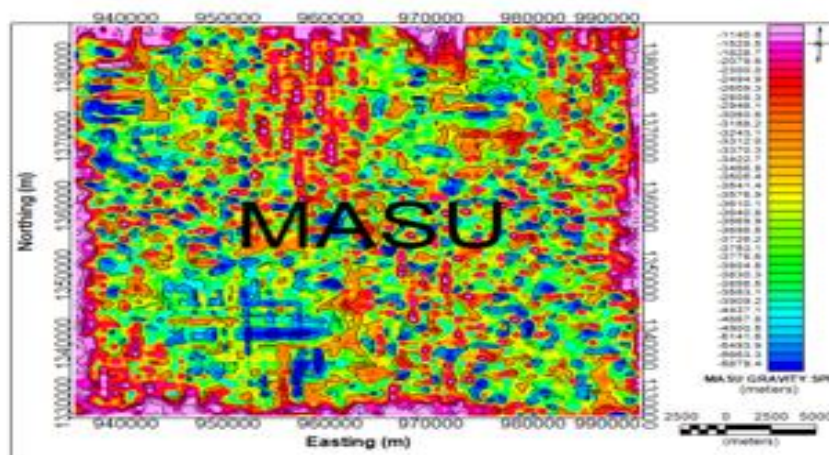(a) Total Magnetic Intensity (TMI) Map of Masu

(b) Bouguer Gravity Map of Masu
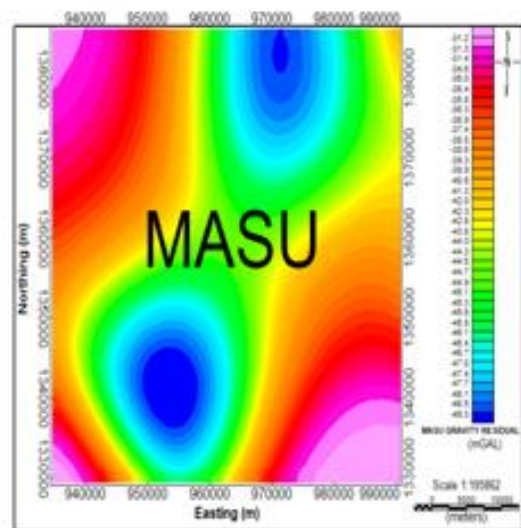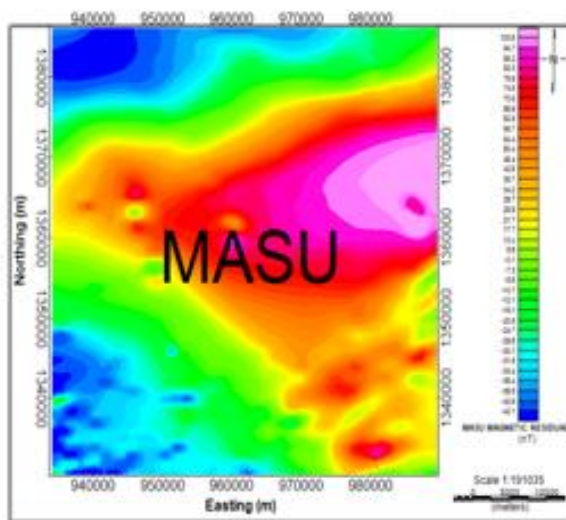
(c) Residual Magnetic Map of Masu

(d) Residual Bouguer Anomaly Map of Masu

Figure 2: Maps of qualitative interpretation of aeromagnetic and aerogravity data for Masu

(a) Aeromagnetic Source Parameter Imaging (SPI) Map of

(b. Aerogravity Source Parameter Image (SPI) Map of Masu

Figure 3: SPI maps of aeromagnetic and aerogravity Depth Estimation in Masu

Table 2: Depth estimates of the first and second magnetic layers for the 9 spectral cells and their coordinates.

| S/N	SPECTRAL BLOCKS/CELLS	C0-0RDINATES (m)		DEPTH SOURCE VALUE (km)	
	SECTIONS	X(Easting)	Y(Northing)	DEEP(D_1)	SHALLOW(D_2)
	1	943234.3	1339903	3.571	0.661
	2	961567.3	1339903	3.628	0.857
	3	979900.3	1339903	2.941	0.970
	4	943234.3	1358236	5.291	1.167
	5	961567.3	1358236	4.409	0.887
	6	979900.3	1358236	6.173	0.852
	7	943234.3	1376569	3.968	0.794
	8	961567.3	1376569	3.685	0.909
	9	979900.3	1376569	4.039	1.080
AVERAGE DEPTH				4.189	0.909

Table 3: Depth estimates of the first and second gravity layers for the 9 spectral cells and their coordinates.

S/N	SPECTRAL BLOCKS/CELLS	C0-0RDINATES (m)		DEPTH SOURCE VALUE (km)	
	SECTIONS	X(Easting)	Y(Northing)	DEEP(D_1)	SHALLOW(D_2)
1	1	943234.3	1339903	4.329	1.240
2	2	961567.3	1339903	5.896	0.907
3	3	979900.3	1339903	2.822	0.543
4	4	943234.3	1358236	3.571	0.361
5	5	961567.3	1358236	2.557	0.388
6	6	979900.3	1358236	2.092	0.493
7	7	943234.3	1376569	4.365	0.825
8	8	961567.3	1376569	4.233	0.767
9	9	979900.3	1376569	3.472	0.517
AVERAGE DEPTH				3.704	0.671
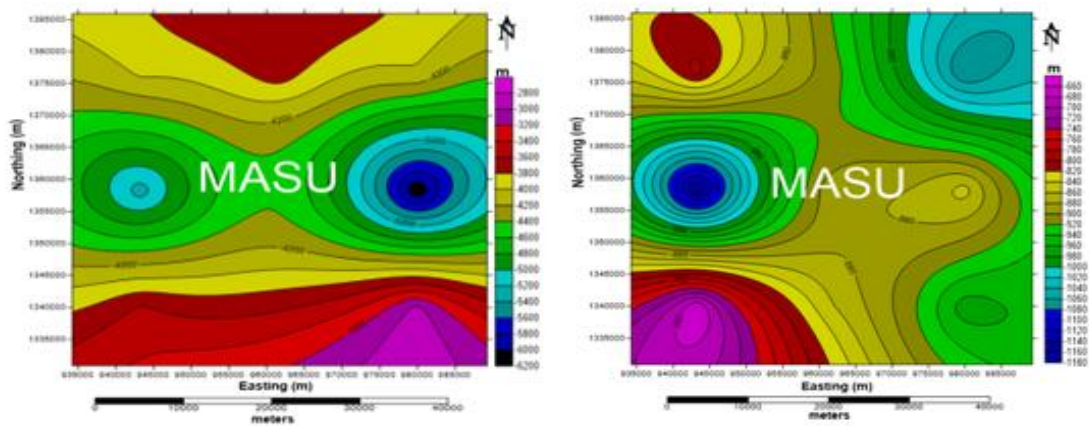
(a) Magnetic deep depth to basement map
(contour interval 200m)

(b) Magnetic shallow depth to basement map
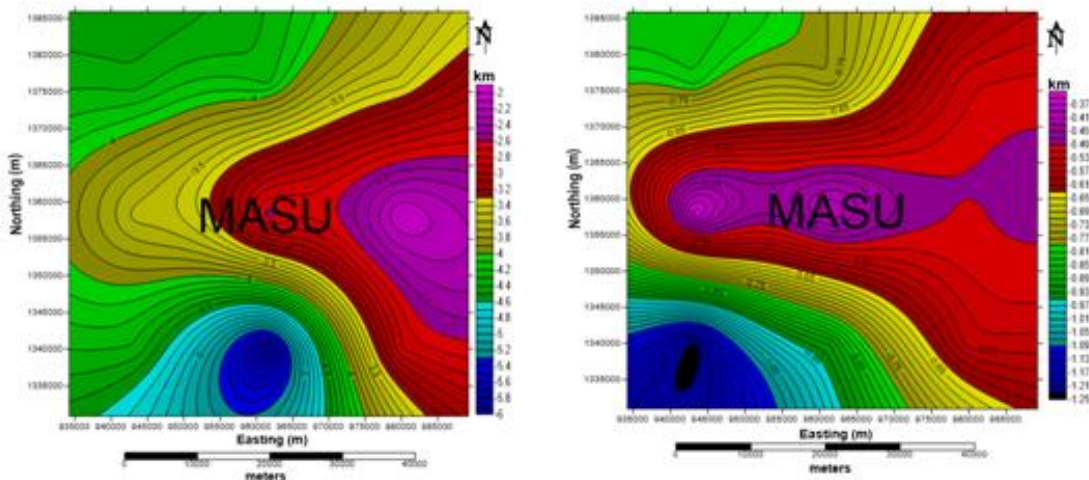
(c) Gravity deep depth to basement map
(contour interval 0.1 km).

(d) Gravity shallow depth to basement map
(contour interval 0.02 km)

Figure 4: 2D Contour maps of shallow and deep depths to basement of Masu

IV. Discussion

From the qualitative interpretation (Fig, 2a), it could be observed that the magnetic anomalies of the area range from- 42.4 to 237.6 nT. The area is marked by the high (pink and red colours) and low (blue colour) magnetic signatures. Consequently high magnetic intensity is observed in the central and eastern parts of the study area, while, the northern and southwestern parts of the area are marked by low magnetic intensity. The

variation in magnetic field intensity could be as a result of degree of strike, variation in depth, difference in magnetic susceptibility, differences in lithology, dip and plunge.[27]

On the other hand, it is noticed from the Bouguer gravity map (Fig. 2b) that the Bouguer anomaly of the area varies from -50.5 to -28.3 mGal. Low gravity anomalies are observed in the north central and southern parts with its minimum value appearing in the southwestern part of Masu. This suggests the existence of sedimentary rocks, since sedimentary rocks are characterized by low density values. High gravity anomalies are observed in the east with its maximum in southeast; small portion of it appears in the northwest and southwest. These high gravity anomalies could be attributed to intrusion of dense metamorphic rocks.[9]

The 2D residual magnetic map (Fig. 2c) of the study area shows magnetic anomalies ranging from -42.1 to 103.6 nT. This indicates the study area as predominantly of high residual magnetic anomalies and small area of low residual magnetic anomalies. This implies that the area is more of intrusive bodies. High residual magnetic anomaly is observed in the east and decreases towards the northwest and the southwest axes. This could be due to near surface rocks containing large magnetic response. Low residual magnetic anomaly values appear in the northwest and southwest of the study area. This could likely be due to the presence of sedimentary rocks (likely sandstones and limestone) or weak magnetic bodies in the area. This agrees with the work of [28] who observed that high residual magnetic intensity in most part of Chad basin is caused by near surface rocks. The residual magnetic map agrees well with the total magnetic intensity map, thereby showing that the area is more of residual magnetic anomalies than the regional magnetic anomalies.

Residual gravity map of Masu (Fig.2d) reveals that the residual gravity anomalies of the study area vary from - 49.3 to - 31.2 mGal. High gravity anomalies which correspond to region with high density contrast beneath the surface is seen in the northwest, southwest and southeast, while low gravity anomalies which correspond to regions of low density contrast are observed in the southwest and northeast of Masu. The high gravity anomaly in the area could be attributed to intrusion of metamorphic rock s (likely marble), while low gravity anomalies could be attributed to sediments in the study area.

The negative sign shown on the source parameter imaging (SPI) legends of Figures 3(a and b) depicts the depths of buried potential field bodies, which may be deep seated basement rocks or near surface intrusive. The pink and red colours generally indicate areas occupied by shallow bodies, while the blue colour depicts areas of deep lying potential field bodies. The depths estimated from source parameter imaging using aeromagnetic data of Masu range from 479.9 to 6507.6 m. The deep depths range from 3856.3 to 6507.6 m, with average of about 5196.8 m, while, the shallow depths range from 479.9 to 1397.7 m, with average of about 897.5 m. Furthermore, from the map it is shown that the southern part of the area is dominated by shallow depths; while the central region and parts of the north are dominate by deep depths. This is an indication that shallow magnetic bodies could be obtained in the southern part of the area, while deep lying magnetic bodies could be obtained in the central and the northern parts of the area.

On the other hand, the estimated depths from source parameter imaging using aerogravity data vary from 1140.6 to 5879.4 m. Areas of deep lying gravity bodies could be found from the depths of about 4437.1 to 5879.4 m, with average of about 5153m, while shallow depths in the area range from 1140.5 to 3158.7 m with average of about 2354.0 m. It is observed that both the deep and shallow depths are scattered all over the area. However, the shallow depth is more pronounced at the edges of the map. This indicates that shallow and deep lying gravity bodies could be obtained all over the study area.

The results obtained from aeromagnetic source parameter imaging closely agrees with that of the aerogravity source parameter imaging. These results confirm the works of other researchers, who have investigated basement depths in other parts of the Nigerian sector of Chad Basin[12, 34, 35]. On the other hand, observation from Table 2 reveals that Masu area has two main magnetic sources depths. These depths are the deep and shallow magnetic depths. The deeper magnetic depth lie at depths that vary between 2.941 and 6.173 km with an average of depth of about 4.189 km, while the shallow magnetic depths ranges from 0.661 to 1.167 km, with an average depth of 0.909 km. The shallow depth in the area may be attributed to the effect of magnetic bodies that intruded into the sedimentary cover, while the deep depth could be as result of the influence of basement rocks. Meanwhile, the deep depth to magnetic basement map (Fig.4a) of Masu reveals that areas at the extreme south and small area at the extreme north has the shallowest magnetic depth, while the area with the deepest magnetic depth is in the eastern area of the map. The shallow magnetic depth to basement (Fig. 4b) on the other hand shows that the southwest and north-western parts of the area is shallowest , while it is deep in the northeast and at the western parts of the area. The average magnetic depth of 4.189 km represents the depth to basement or sedimentary thickness of the area. This spectral result obtained in the area, somehow has little discrepancies with the results obtained by other researchers such as [5] who obtained the depth to basement of 4.5 km in Kam area and [6] who obtained the depth to basement of 4. 246 km in Abakaliki and Ugep. The discrepancy may be due to differences in the location of the study areas.

Using gravity data, observation from Table 3 indicates that the deep depth of the area vary between 2.092 to 5.896 km, with an average depth of 3.704 km, while the shallow depth ranges from 0.361 to 1.240 km,

with an average depth of 0.671 km. The 2-D deep depth to basement map (Fig.4c) shows that the deep depth in the area is shallowest (purple colour) in the east and decreases towards the western part of Masu, however, it is deepest (black colour) in the southern part of the area. The shallow depth to basement map (Fig.4d) on the other hand, indicates that the shallow depth is low in the east and spread through the central region to the western part of the area, while it is high in the south-western part of the area.

V. Conclusion

The depth to basement from the two methods seems to be equal, though the spectral depth is higher than source parameter imaging. Therefore, the highest sedimentary thicknesses obtained from both methods in this work are sufficient enough for hydrocarbon accumulation based on the assertion made by [39] that the minimum thickness of the sediment required for the commencement of oil formation from marine organic remains would be 2300 m (2.3km). This implies that Masu has the potential for hydrocarbon accumulations within the depths of about 2354.0 - 5153 m estimated in this work.

References

[1]. Adekoya, J.A; Ola, P.S and Olabole, S.O. (2014). Possible Bornu Basin Hydrocarbon Habitat A reviews. *International Journal of Geosciences* 5: 983-996.

[2]. Aderoju, A.B., Ojo, S.B., Adepelumi, A.A. and Edino, F. (2016). A reassessment of hydrocarbon prospectivity of the Chad Basin, Nigeria, using magnetic hydrocarbon indicators from High – Resolution Aeromagnetic imaging. *Ife Journal of Science.*18 (2): 503-520.

[3]. Adewumi, T. Saloko, K.A., Salami, M.K., Mohammed, M.A. and Udensi, E.E.(2017). Estimation of Sedimentary Thickness using Spectral Analysis of Aeromagnetic Data over part of Borno Basin, North east, Nigeria. *Asian Journal of Physical and Chemical Sciences 2(1): 1-8.*

[4]. Ajana, O.; Udensi, E.E.; Momoh, M.; Rai, J.K. and Muhammad, S.B. (2014). Spectral Depths Estimatof Subsurface in Parts of Chad Basin Northeastern Nigeria. *Journal of Applied* Geology *and Geophysics.* 2(2):58-6

[5]. Alagbe, O.A. (2015) Depth Estimation from Aeromagnetic data of Kam. *International journal of Advanced Research in physical science (IJARPS) 2(1): 37- 52*

[6]. Alasis T. K., Ugwu G. Z. and Ugwu, C. M. (2017). Estimation of Sedimentary Thickness using Trough, Nigeria *International Journal of Physical Sciences.* 12(21): 270 – 279.

[7]. Ali, S. and Orazulike, D.M. (2010). Well logs – Derived Radiogenic Heat Production in the Sediments of the Chad Basin, North – East Nigeria, *Journal of Applied Science* 2: 1-5.

[8]. Avbovbo. A. A.; Ayoola, E.O. and Osahon, G.A. (1986). Depositional and Structural Styles in Chad Basin of Nigeria. Bulletin American Association Petroleum Geologists.70 (121):1787-1798.

[9]. Ayad, A and Bakkali, S. (2017). Interpretation of Potential gravity anomalies of Ouled Abdoun Phosphate basin (central Morocco). *Journal of materials and Environmental science, 8(9): 3391-3397*

[10]. Barber, W. (1965) Pressure Water in the Chad formation of Borno and Dikwa Emirates, NE Nigeria. Bulletin Geological Survey of Nigeria.(35):138

[11]. Blakely, R.J. (1988). Curie Temperature Analysis and Tectonic Implications of Aeromagnetic Data from Nevada. *Journal of Geophysical Research.* 93 (B10): 11817 – 11832.

[12]. Chinwuko, A.I.; Onwuemesi, A.G.; Anakwuba, E.K.; Okeke, H.C.; Onuba, L.N.; Okonkwo, C.C. and Ikumbur, E.B. (2013): Spectral Analysis and Magnetic Modeling over Biu-Damboa, North Eastern Nigeria. *IOSR Journal of Applied Geology and Geophysics.* 1(1):20 -28

[13]. Dobrin M.B (1976): Introduction to Geophysical Prospecting 3rd Edition, MC-Grew Hill Co, New York, 630 pp.

[14]. Emmanuel, K., Anakwuba, T; Ajana, G., Onwuemesi, P; Augustine, I., Chinwko, K and Onuba, L.N. (2011). The Interpretation of Aero magnetic Anomalies over Maiduguri-Dikwa Depression, Chad Basin Nigeria, Structural *view Archives of Applied Science Research* 3(4): 499-508.

[15]. Fagbenle, P.K (2016). Hydrocarbon Potentials Prospects in Chad Basin. Daily Trust News Paper of 25th July vol. 9 no.24 Pp 4.

[16]. Hsu, N.C.; Herman, J. R.; Bhartia, P.K.; Seftor, C.J.; Torres, O.; Thompson, A.M.; Gleason, J.F.; Eck, T.F., and Holben, B.N. (1996). Detection of biomass burning smoke from TOMS measurement. Geophysics Research letters, 23,745- 748.

[17]. Kasidi, S. and Nur, A. (2012). Curie Depth Isotherm Deduced from Spectral Analysis of Magnetic Data over Sarti and Environs of North-Eastern, *Nigeria Scholarly Journals of Biotechnology.* 1(3): 49-56.

[18]. Kwaya, M.Y., Kurowska, E., Alagbe, S.A., Ikpokonte, A.C. and Arabi, A.S. (2013).Evaluation of Depth to Basement Complex and Cernozoic Uniformity from Seismic Profiles and Boreholes in the Nigerian Sector of the Chad Basin, *Journal of Earth Science and Geotechnical Engineering.* 3 (2): 43-49.

[19]. Lawal, T.O. and Nwankwo, L.T.(2014).Wave let Analysis of High Resolution Aeromagnetic Data over Part of Chad Basin, Nigeria. *Ilorin Journal of Science* 1: 110-120.

[20]. Matheis, G. (1976). Short review of the geology of Chad Basin in Nigeria, Elizabethan publication company Lagos, Nigeria, 289-294.

[21]. Mijinyawa, A. B.; Bhattacharya, S.K.; Mournouni, A.; Mijinyawa, S. and Mohammed, I. (2014). Hydrocarbon potentials, thermal and Burial History in Herwa-1 from the Nigerian sector of the Chad Basin: An implication of 1-D Basin modeling study. *Research Journal of Applied Sciences, Engineering and Technology* 6(6): 961-968

[22]. Nabighian, M. N. (1972). The Analytic Signal of Two Dimensional Magnetic Bodies with Polygonal Cross-section: Its Properties and Use for Automated Anomaly Interpretation. *Geophysics.* 37 (3): 507- 517.

[23]. Nwankwo, C.N.; Anthony S.; Ekine, P.; Nwasu. K, and Leonard. I. (2012). Estimation of

the Heat Flow Variation in the Chad Basin Nigeria. *Journal of Applied Sciences EnvironmentaManagement.4:28-34.*

[24]. Nwankwo, C.N. and Ekine, A.S. (2009). Geothermal Gradients in the Chad Basin, Nigeria from Bottom hole temperature Logs. *International Journal of physical sciences.* 4 (12): 777 – 783.

[25]. Nwosu, L. and Emujakporu, G. (2017). Porosity Depth Estimation in Chad Basin Nigeria lJSRM *International Journal of Sciences and Research Methodology.* 5(4): 111-121.

[26]. Obaje, N. G. (2009). Geology and Mineral Resources of Nigeria, Berlin Springer publishers

[27]. Obiora, D.N.; Ossai, M.N. and Okwohi, E. (2015).   A Case Study of Aeromagnetic Data Interpretationof Nsukka Area, Enugu state,Nigeria for hydrocarbon Exploration. *International Journal of Physical Science.* 10 (17): 503-519.

[28]. Oghuma, A.A.; Obiadi, I.I. and Obiadi, C.M. (2015). 2- D Spectral Analysis of Aeromagnetic Anomalies over Parts of Montu and Environs, Northeastern, Nigeria. *Journal of Earth Science and Climatic Change.* 6:8-14.

[29]. Odebode, M. O. (2010) A handout on geology of Borno (Chad) Basin Northeastern   Nigeria.

[30]. Okosun, E.A. (1995) Review of Borno Basin. *Nigerian Journal of mining and geology 31(2):113-172.*

[31]. Okpikoro, F.E. and Olorunniwo, M. A. (2010). Seismic Sequence Architecture and Structural Analysis of North–Eastern, Nigeria Chad (Bornu) Basin, Journal *of Earth Science* 5(2): 1-9

[32]. Onwuemesi, A.G. (1997). One-Dimensional Spectral Analysis of Aeromagnetic Anomalies and Curie point Depth Isotherm in the Anambra Basin of Nigeria. *Journal of Geodynamics.* 23(2):95-107.

[33]. Rabeh, T. (2009). Prospecting for the Ferromagnetic Mineral Accumulations Using the Magnetic Method at the Eastern Desert, Egypt.. *Journal of Geophysics and Engineering.* (4): 401 – 411.

[34]. Salako, K. A. (2014). Depth to Basement Determination Using Source Parameter Imaging (SPI) of Aeromagnetic Data: An Application to Upper Benue Trough and Borno Basin, Northeast, Nigeria. *Academic Research International,* 5(3): 74-86.

[35]. Sanusi, Y.A. and Likkason, O.K. (2016). Angular Spectral Analysis and low pass filtering of Aeromagnetic Data over Western parts of Nigerian Chad (Borno) Basin, Nigeria. Nigerian Journal of Basic and Applied Science 24(2):73- 84.

[36]. Shuey, R.T.; Schellinger, D.K.; Tripp, A.C, and Alley, L.B. (1977). Curie Depth Determination from Aeromagnetic Data Spectral Analysis. *Geophysics Journal of the Royal Astronomical society. 50 (1): 73-101.*

[37]. Spector, A. and Grant. F. (1970). Statistical Models for Interpreting Aeromagnetic data *International Journal of Geophysics*, 35 (2): 293 – 302.

[38]. Thurston, J.B. and Smith, R.S. (1997). Automatic Conversion of Magnetic data to Depth dip and Susceptibility Contrast Using the SPI Methods. *International Journal of Geophysics*. 62 (3): 807 – 813.

[39]. Wright, J. B.; Hastings, D.; Jones, W. B.; Williams, H.R. (1985). Geology and Mineral resources of West Africa. George Allen and Urwin, London.